Transport and Communications Science Journal, Vol. 76, Issue 07 (09/2025), 980-994

Transport and Communications Science Journal

EFFECTS OF COMPACTION PARAMETERS ON COMPRESSIVE STRENGTH OF ROLLER-COMPACTED CONCRETE USING GROUND GRANULATED BLAST-FURNACE SLAG

Lam Ngoc Tra My *

Department of Transportation Engineering, Faculty of Civil Engineering, Ho Chi Minh City University of Technology and Education, No 1 Vo Van Ngan Street, Ho Chi Minh City, Vietnam

ARTICLE INFO

TYPE: Research Article
Received: 17/02/2025
Revised: 07/08/2025
Accepted: 09/09/2025
Published online: 15/09/2025
https://doi.org/10.47869/tcsj.76.7.5
* *Corresponding author*
Email: mylnt@hcmute.edu.vn

Abstract. Roller-compacted concrete (RCC) is a zero-slump concrete in which compaction plays a critical role in determining strength and durability. This research investigated the effects of compaction parameters on the compressive strength of RCC incorporating varying contents of ground granulated blast-furnace slag (GGBFS). Different compaction techniques, including the vibrating hammer and Proctor hammer, were evaluated along with the influence of compaction energy levels—low, standard, and high. Compressive strength tests were conducted at 7, 28, and 56 days on RCC specimens compacted using both methods. Results showed that replacing cement with GGBFS reduced compressive strength at 7 days but improved it at 28 and 56 days. Specimens compacted with the vibrating hammer consistently exhibited higher compressive strength than those compacted using the Proctor hammer. Insufficient compaction energy in the Proctor method led to a general reduction in strength across all mixtures. Conversely, increasing compaction energy slightly decreased the strength of Group A mixtures, likely due to aggregate breakage and disruption of optimal packing. In contrast, the Group B mixtures showed improved strength at higher compaction energy, likely because the energy level was sufficient to achieve maximum density. However, when the compaction energy exceeded the optimal level, a decline in strength was observed.

Keywords: roller-compacted concrete, ground granulated blast-furnace slag, vibrating hammer, modified Proctor method, compaction energy, compaction method.

1. INTRODUCTION

Roller-compacted concrete (RCC) is a stiff, no-slump concrete commonly used in the construction of dams and pavements. The compaction process plays a critical role in ensuring the quality and performance of RCC, as it rearranges the aggregate particles, reduces voids, and increases overall density. In field applications, the use of multiple roller types is essential for achieving effective compaction. Typically, a combination of static, vibratory, and pneumatic rollers is employed to compact RCC on-site. In contrast, laboratory compaction of RCC specimens can be performed using equipment such as a vibrating hammer, vibrating table, gyratory compactor, or the modified Proctor method. Selvam et al. [1] reported that the interparticle distance of aggregates in RCC specimens compacted using either a vibrating table or a gyratory compactor is comparable to that observed in field-compacted RCC. However, Sengun et al. [2] stated that specimens prepared using the vibrating table method exhibited the lowest strength compared to those compacted by other methods. Additionally, the gyratory compactor method is considered complicated for preparing RCC specimens in the laboratory. According to a study by Williams [3], the density of RCC compacted with a gyratory compactor increased as the actual moisture content of the mixture increased, which prevented the determination of optimum moisture content. Among the available laboratory methods, the vibrating hammer method conforms to ASTM C1435 [4], is the most commonly used for preparing RCC specimens. Nevertheless, Selvam and Singh [5] demonstrated that RCC specimens prepared using the vibrating hammer method tended to overestimate strength when compared to specimens produced under field conditions. In contrast, specimens compacted using the modified Proctor method exhibited strength values more representative of field performance [5]. However, there is a lack of specific standards governing the preparation of RCC specimens in the laboratory using the modified Proctor method.

Blast furnace slag is a by-product generated during the production of pig iron. Once ground into a fine powder, ground granulated blast-furnace slag (GGBFS) is commonly used as a cement replacement material due to its chemical composition. The primary chemical components of GGBFS are calcium, silica, and alumina oxides. Oner and Akyuz [6] reported that increasing the GGBFS substitution ratio led to higher compressive strength in concrete incorporating GGBFS. Similarly, Rao et al. [7] observed that the inclusion of GGBFS in RCC resulted in a decrease in compressive strength at 3 days. However, as the curing period extended from 7 to 28 days, the compressive strength of RCC incorporating GGBFS increased by 39% to 63%. In addition, the split tensile strength at 90 days improved from 28% to 51%, depending on the GGBFS content in the mixtures. Additionally, replacing 20% to 40% of cement with GGBFS improved the permeability resistance of roller-compacted concrete pavement at 90 days [8]. Moreover, the roller-compacted concrete pavement mixtures containing GGBFS exhibited reduced porosity and water absorption compared to the control at 90-day ages [8]. The benefits of incorporating GGBFS in RCC highlight the need for further investigation. Robalo et al. [9] also noted that concrete with a low cement content exhibits reduced cohesion and consistency, which demands higher compaction energy to achieve adequate strength. Therefore, the main objectives of this research are:

1. To compare the compressive strength of RCC specimens containing GGBFS, prepared using the vibrating hammer and modified Proctor methods, under both normal and low cementitious dosages.
2. To evaluate the compressive strength of RCC containing GGBFS, compacted using varying Proctor hammer blows (i.e., low, standard, and high levels).

2. EXPERIMENTAL PROGRAM

2.1. Materials

This research employed original Portland cement (OPC) Type I (Fig. 1a), produced by Nghi Son Company, which complies with ASTM C150 [9]. The compressive strength of the OPC was measured according to ASTM C109 [10] and recorded values of 15.3 MPa, 27.6 MPa, 34.2 MPa, and 57.2 MPa at 1, 3, 7, and 28 days, respectively. The fineness of the OPC determined using the Blaine air-permeability apparatus [11], was 389 m²/kg. The initial and final setting times, tested following ASTM C191 [12], were 110 minutes and 170 minutes, respectively. The chemical composition of the OPC, analysed via X-ray fluorescence (XRF), is presented in Table 1. Moreover, the X-ray diffraction (XRD) results of OPC, as shown in Fig. 2, identified alite and belite as the primary crystalline phases present in the cement.

Table 1. The properties of the cement and GGBFS.

Properties	Unit	Cement	GGBFS
Physical properties			
Blaine fineness	m^2/kg	389	528
Density	g/cm^3	3.1	2.9
Initial setting time	min	110	
Final setting time	min	170	
Mechanical properties			
Compressive strength	MPa		
1 day		15.3	-
3 days		27.6	-
7 days		34.2	-
28 days		57.2	-
Chemical composition			
MgO	%	1.8	5.4
CaO	%	63.0	37.1
K_2O	%	0.1	0.7
SO_3	%	2.3	1.6
SiO_2	%	20.7	41.9
Al_2O_3	%	4.5	10.1
Fe_2O_3	%	3.3	0.2

GGBFS, classified as S95 (Fig. 1b) according to TCVN 11586 [13], was used in this study. The GGBFS had a density of 2.9 g/cm³ and a fineness of 528 m²/kg. Its slag activity index reached 85.2% at 7 days and 102.5% at 28 days. The chemical composition of the GGBFS, determined by XRF analysis, is presented in Table 1. Based on these results, the GGBFS used in this study met all the requirements specified in TCVN 11586 [13]. Furthermore, the mineralogical composition of the GGBFS was analysed using XRD. As shown in Fig. 3, the results indicate that the GGBFS primarily consists of amorphous aluminosilicate compounds.

Fig. 1 Cementitious materials used to produce RCC.

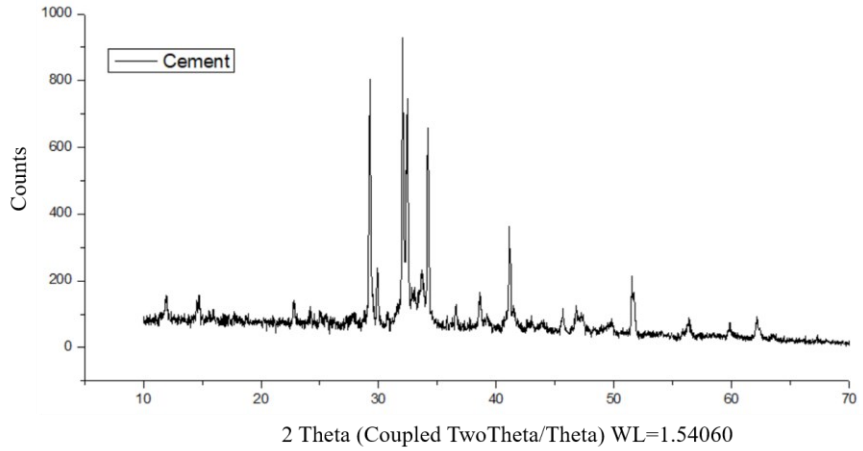

Figure 2. XRD plot of the OPC.

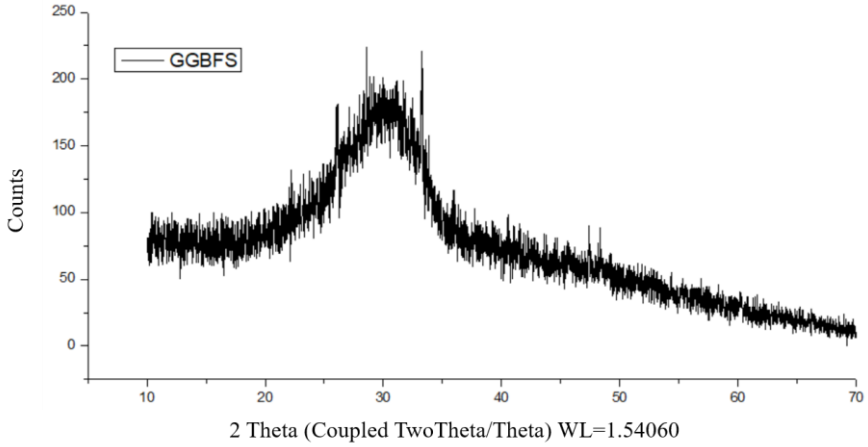

Figure 3. XRD plot of the GGBFS.

Natural crushed stone (Fig. 4a) and river sand (Fig. 4b) were used as coarse and fine aggregates, respectively. Their physical properties are summarized in Table 2. The particle size distribution of the aggregates is illustrated in Fig. 5. As shown, the grading of the aggregate particles aligns well with the 0.45-power curve, which is highly recommended by the American Concrete Pavement Association [14] for the preparation of RCC.

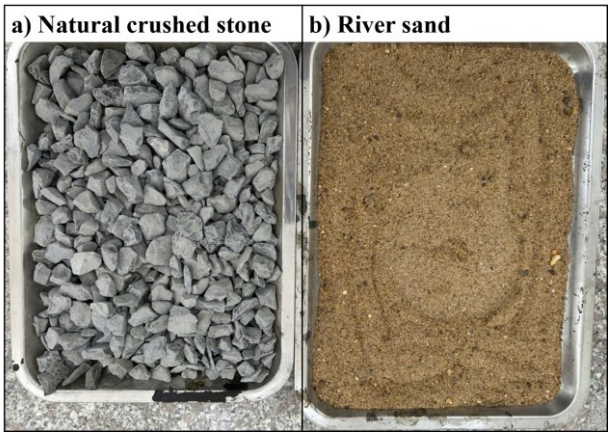

Fig. 4 Aggregates used to produce RCC.

Table 2. The physical properties of aggregates.

	Specific gravity	Bulk density (kg/m^3)	Water absorption (%)
River sand	2.65	1502	1.2%
Natural crushed stone	2.75	1447	0.5%

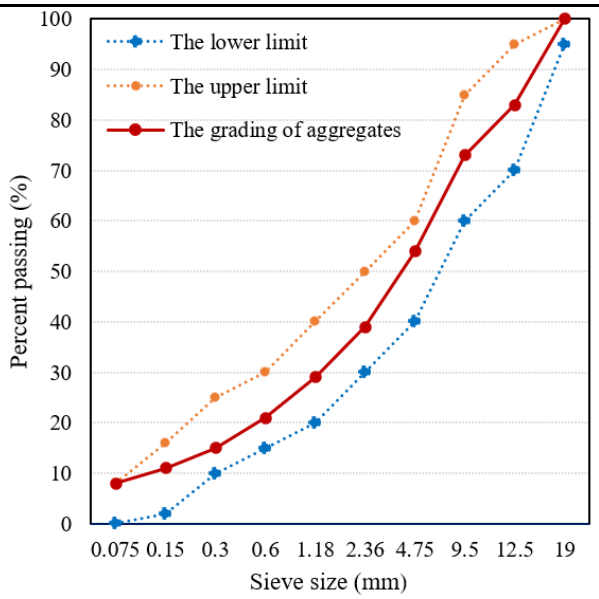

Figure 5. The grading of the aggregates.

2.2. Mixture proportioning of RCC

The Institute for Transportation of Iowa State University reported that the cementitious material content in RCC typically ranges from 10% to 17% of the dry weight of the concrete mixture [15], equivalent to 208 to 356 kg per metric ton of RCC. The specific amount of cementitious material depends on the target compressive strength of the RCC at 28-day age. In this study, two levels of cementitious material content were selected. At Level 1 (group A), 300 kg of cement per metric ton of RCC was used to achieve a target compressive strength of 50 MPa at 28 days. At Level 2 (group B), 200 kg of cement per metric ton of RCC was used to reach a target compressive strength of 30 MPa at 28 days. To evaluate the effects of GGBFS on the compressive strength of RCC, the weight of OPC was partially replaced with GGBFS at three levels: 15%, 30%, and 45%.

Table 3. The mixture proportions per 1 metric ton of RCC.

Group	ID. mixtures	Cementitious materials (kg)		Aggregates (kg)	
		OPC	GGBFS	Natural sand	Crushed stone
A	ACT	300	0	900	1080
	AG15	255	45	900	1080
	AG30	210	90	900	1080
	AG45	165	135	900	1080
B	BCT	200	0	960	1150
	BG15	170	30	960	1150
	BG30	140	60	960	1150
	BG45	110	90	960	1150

The aggregates in RCC typically account for 75% to 85% of its total volume. In this study, the aggregate content was calculated based on the assumption of achieving the densest packing in the RCC mixture. Hashemi et al. [16] recommended optimizing the coarse-to-fine

aggregate ratio at 1.2. Following these guidelines, the mixture proportions for the RCC were determined and are presented in Table 3.

The water contents of the RCC mixtures were determined using the soil compaction method. In this approach, the relationship between dry unit weight and water content is established by compacting multiple specimens at varying moisture levels. The modified Proctor test, following ASTM D1557 [17], was employed for this purpose. For each RCC mixture, six specimens were prepared with six different moisture contents: 5%, 6%, 7%, 8%, 9%, and 10% (as shown in Table 4). The moisture content of each mixture was calculated using Eq. (1).

$$W(\%) = \frac{m_w}{m_{cem} + m_{agg}} \times 100 \quad (1)$$

Where W is the moisture content of the mixture (%); m_w is the weight of water in the mix (kg); m_{cem} is the weight of cementitious materials (including OPC and GGBFS) (kg); and m_{agg} is the weight of aggregates at an oven-dried condition in the mixture (kg).

The cementitious materials (including OPC and GGBFS) and aggregates were first mixed in a mixing machine under dry conditions for approximately 2 minutes. Subsequently, water was added to the mixture, and mixing was continued for an additional 2 minutes. According to ASTM D1557 [17], the 6-inch diameter (152.4 mm) mold is compacted in five layers, with 56 blows applied to each layer. Therefore, after mixing, the RCC mixture was placed into the modified Proctor mold in five layers, and each layer was compacted with 56 blows following the standard procedure. Following compaction, the wet unit weight of the RCC was measured. The dry unit weight of the RCC at a specific moisture content was then calculated using Eq. (2). Finally, the relationship between the dry unit weight and the water content of the RCC was established and plotted as a compaction curve.

$$\gamma_{dry} = \frac{\gamma_{wet}}{1 + W} \quad (2)$$

Where γ_{dry} is the dry unit weight of RCC (kg/m^3); γ_{wet} is the wet unit weight of RCC (kg/m^3).

Table 4. The water content prepared for the modified Proctor test

Group	ID. mixtures	Water (kg)					
		W = 4%	W = 5%	W = 6%	W = 7%	W = 8%	W =9%
A	ACT	91.2	114	136.8	159.6	182.4	205.2
	AG15	91.2	114	136.8	159.6	182.4	205.2
	AG30	91.2	114	136.8	159.6	182.4	205.2
	AG45	91.2	114	136.8	159.6	182.4	205.2
B	BCT	92.4	115.5	138.6	161.7	184.8	207.9
	BG15	92.4	115.5	138.6	161.7	184.8	207.9
	BG30	92.4	115.5	138.6	161.7	184.8	207.9
	BG45	92.4	115.5	138.6	161.7	184.8	207.9

2.3. Sample preparation and testing program

After the optimum water content for each mixture was determined from the compaction curve, the RCC mixtures were prepared using this optimum water content. Cubic specimens were then cast to evaluate the compressive strength of RCC following TCVN 3118 [18].

The testing program for this research is illustrated in Fig. 6. Two compaction methods were employed for specimen preparation: vibrating hammer compaction and Proctor hammer

compaction. After mixing, the RCC mixtures were compacted using a vibrating hammer (Fig. 7a) for 20 seconds per layer following ASTM C1435 [4].

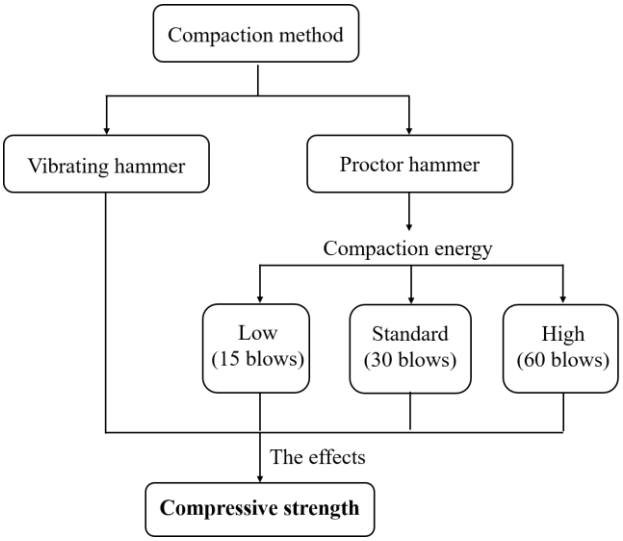

Figure 6. The testing program.

Following ASTM D1557 [17], the standard compaction procedure for a 6-inch diameter (152.4 mm) mold involves compacting the mixture into five layers with 56 blows per layer. Based on this, the number of blows was recalculated to ensure an equivalent compaction effort for 100 mm cubic molds. The RCC mixtures were placed into the cubic molds in two layers and compacted with 30 blows per layer using a Proctor hammer (Fig. 7b) to achieve standard compaction energy, as shown in Fig. 6. Additionally, specimens were compacted at low and high energy levels, corresponding to 15 blows per layer and 60 blows per layer, respectively.

The compressive strength of RCC was determined at 7, 28, and 90 days following TCVN 3118 [18]. Each reported result represents the average value obtained from three specimens. In total, 192 specimens were prepared for this study, as summarized in Table 5.

Additionally, Table 5 presents the abbreviations used for each mixture. For instance, the control specimens compacted using a vibrating hammer are denoted as ACT-V, whereas the control specimens compacted with 30 blows per layer using a Proctor hammer are identified as ACT-PS.

Table 5. The number of specimens and abbreviations for mixtures.

Group	ID. mixtures	Vibrating hammer method	Proctor hammer method		
			Low compaction	Standard compaction	High compaction
A	ACT	9 (ACT-V)	3	9 (ACT-PS)	3
	AG15	9 (AG15-V)	3	9 (AG15-PS)	3
	AG30	9 (AG30-V)	3	9 (AG30-PS)	3
	AG45	9 (AG45-V)	3	9 (AG45-PS)	3
B	BCT	9 (BCT-V)	3	9 (BCT-PS)	3
	BG15	9 (BG15-V)	3	9 (BG15-PS)	3
	BG30	9 (BG30-V)	3	9 (BG30-PS)	3
	BG45	9 (BG45-V)	3	9 (BG45-PS)	3

Figure 7. a) A vibrating hammer, and b) A Proctor hammer.

3. RESULTS AND DISCUSSION

3.1. The optimum water content

Table 6 presents the wet unit weight of RCC after compaction at various moisture contents. Based on Eq. (2), the corresponding dry unit weight of RCC was calculated. Subsequently, the relationship between the dry unit weight and moisture content for each RCC mixture was established, as illustrated in Fig. 8.

Based on Fig. 8, the maximum dry unit weight corresponding to the optimum moisture content for each RCC mixture was determined, as presented in Table 7. As illustrated in Fig. 9, the maximum dry unit weight of RCC containing GGBFS was lower than that of the control mixture. For instance, the maximum dry unit weight of the AG15 mixture, which incorporated 15% GGBFS as a replacement for cement, was 2294 kg/m³ — representing a 0.8% reduction compared to the ACT mixture. Similar reductions were observed in the RCC mixtures containing 30% and 45% GGBFS. This decrease is attributed to the lower specific gravity of GGBFS (2.9 g/cm³) compared to OPC (3.1 g/cm³). Additionally, it was observed that increasing the aggregate content, as seen in Group B mixtures, led to a higher maximum dry unit weight of RCC. Consequently, the RCC mixtures in Group B exhibited a higher maximum dry unit weight than those in Group A.

Table 6. The wet unit weight (γ_{wet}) of RCC.

Group	ID. mixtures	The wet unit weight (γ_{wet}), kg/m^3					
		W = 4%	W = 5%	W = 6%	W = 7%	W = 8%	W = 9%
A	ACT	2341	2402	2450	2468	2483	2470
	AG15	2345	2396	2420	2462	2440	2422
	AG30	2338	2385	2435	2423	2408	2382
	AG45	2315	2361	2410	2392	2365	2347
B	BCT	2370	2442	2485	2530	2551	2540
	BG15	2340	2425	2491	2520	2540	2521
	BG30	2338	2410	2480	2504	2468	2455
	BG45	2315	2390	2460	2510	2410	2347

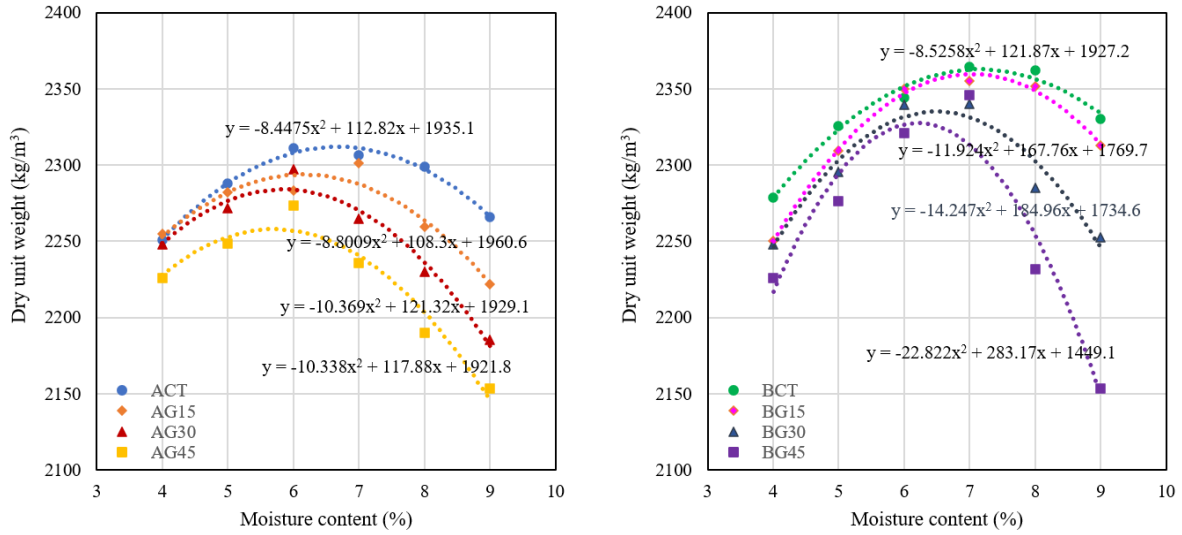

Figure 8. The compaction curves of RCC.

Table 7. The maximum dry unit weight and the optimum moisture content of each RCC mixture

Group	ID. mixtures	The maximum dry unit weight (kg/m³)	The optimum moisture content (%)	The optimum water content (kg)
A	ACT	2312	6.68	152.3
	AG15	2294	6.15	140.2
	AG30	2284	5.84	133.1
	AG45	2258	5.70	130.0
B	BCT	2363	7.15	165.2
	BG15	2360	7.03	162.4
	BG30	2335	6.49	149.9
	BG45	2327	6.20	143.2

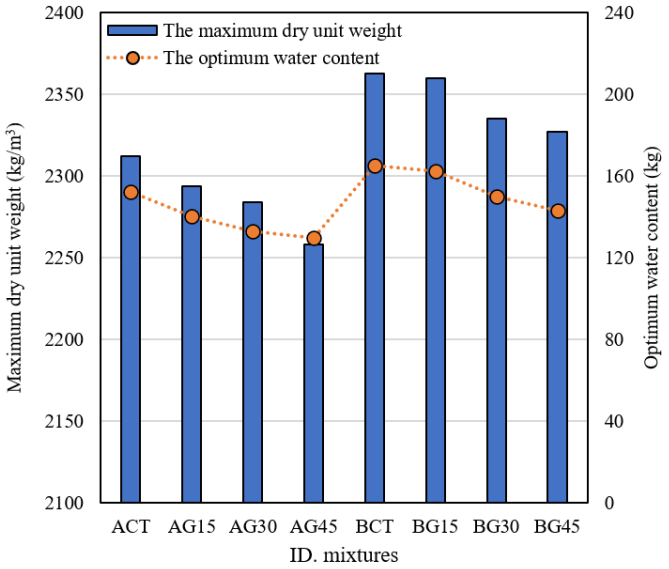

Figure 9. The maximum dry unit weight and the optimum moisture content of RCC.

Additionally, the optimum water content of RCC slightly decreased as the GGBFS replacement level increased. Huiwen et al. [19] demonstrated that GGBFS particles possess

smooth surfaces and spherical shapes, which enable them to act as lubricants within concrete mixtures, thereby enhancing workability [20]. Similarly, Wainwright and Rey [21] observed that the workability of control concrete (without GGBFS) improved from 15 mm to 20 mm or even 40 mm when OPC was replaced with GGBFS at replacement levels of 55% and 85%, respectively.

On the other hand, an increase in the aggregate content of the mixture led to a reduction in workability. Specifically, the aggregates used in Group B weighed 2110 kg/m³, which was higher than the aggregate content in Group A. Consequently, the mixtures in Group B exhibited a higher optimum water content compared to those in Group A. For example, the optimum moisture content for the BCT mixture was determined to be 7.15%, whereas the ACT mixture exhibited an optimum moisture content of 6.68%.

3.2. Effects of GGBFS on compressive strength of RCC at various ages

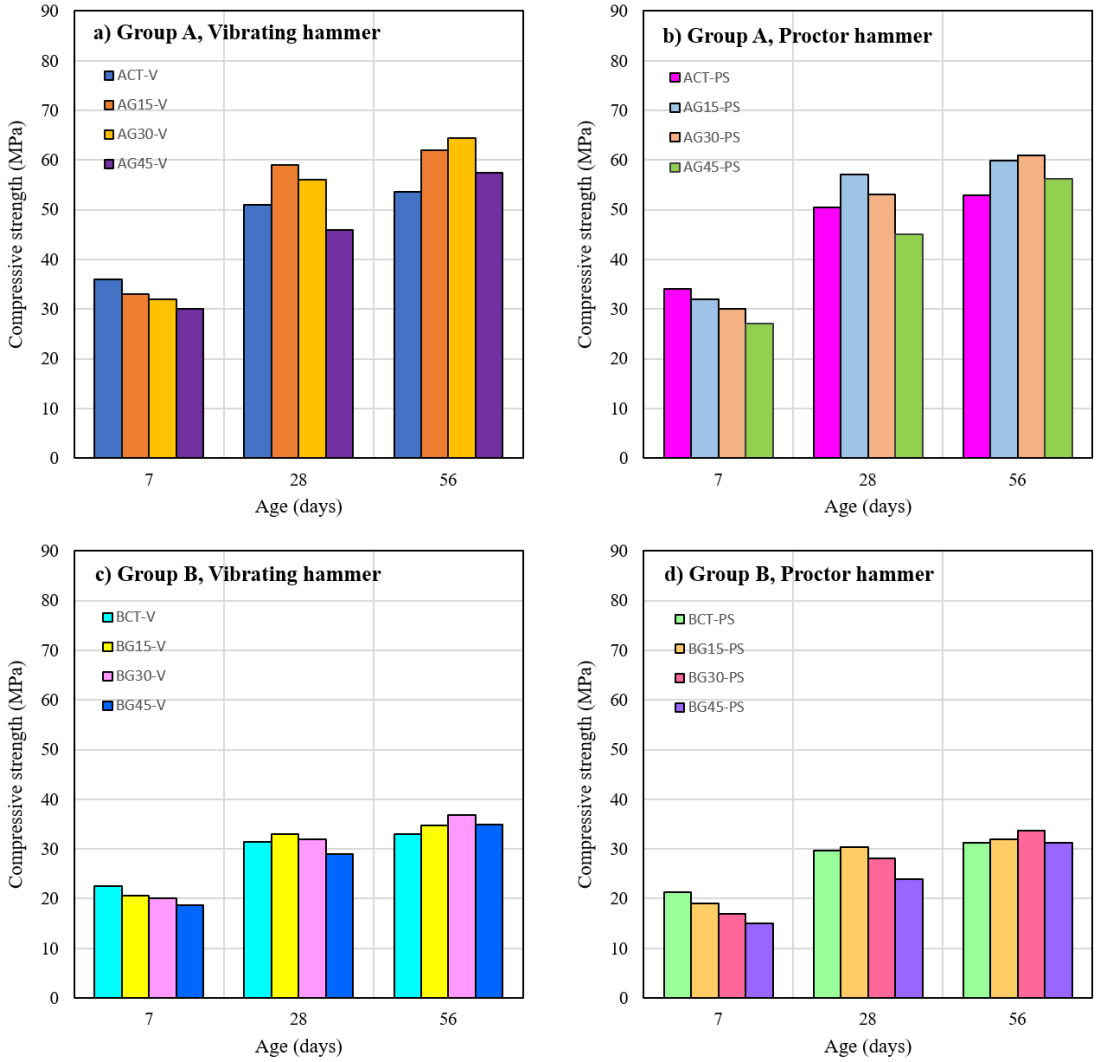

Figure 10. Compressive strength of RCC at various ages.

Fig. 10 presents the compressive strength of RCC at 7, 28, and 56 days. At 28 days, the compressive strength of RCC prepared with 300 kg of cementitious materials ranged from 45 MPa to 57 MPa, depending on the GGBFS replacement level. Meanwhile, the RCC mixtures

containing 200 kg of cementitious materials achieved compressive strengths ranging from 24 MPa to 30 MPa at the same age.

Replacing cement with GGBFS at 15%, 30%, and 45% resulted in a reduction of compressive strength at 7 days across all mixtures. This reduction is attributed to the slower early-age hydration rate of GGBFS compared to cement [22]. The pozzolanic reaction between GGBFS and calcium hydroxide, as expressed in Eq. (3), typically requires more time to contribute significantly to strength development [23]. As a result, at 28 days, the RCC mixture containing 15% GGBFS exhibited the highest compressive strength among the GGBFS-modified mixtures. However, by 56 days, the mixture containing 30% GGBFS surpassed the others, achieving the highest compressive strength at this later age.

$$Ca(OH)_2 + SiO_2 + H_2O \rightarrow CSH \tag{3}$$

Replacing 45% of the cement with GGBFS resulted in a noticeable reduction in compressive strength at 7 days. However, by 56 days, the compressive strength of the RCC mixture containing 45% GGBFS surpassed that of the control mixture. This trend is consistent with the findings reported by Hwang and Lin [24], who observed that the optimal replacement level of GGBFS in mortars was approximately 50%. Similarly, Oner and Akyuz [6] demonstrated that incorporating GGBFS at 55–59% of the total cementitious material significantly enhanced the long-term compressive strength of concrete. Furthermore, GGBFS has been successfully used as a high-volume cement replacement in high-performance concrete [25]. As noted in a study by Guneyisi and Gesoglu [25], replacing 50% to 60% of cement with GGBFS can result in higher compressive strength at 90 days compared to conventional concrete without GGBFS.

3.3. Effects of the compaction method on the compressive strength of RCC

As shown in Fig. 11, all RCC specimens compacted using the vibrating hammer exhibited higher compressive strength at all tested ages compared to those compacted with the Proctor hammer. This enhancement in strength is attributed to the more uniform distribution and denser packing of aggregates, which was achieved through the combined effect of vibration and impact force applied by the vibrating hammer. Selvam et al. [4] reported that RCC specimens compacted using a vibrating hammer exhibited a highly homogeneous aggregate distribution in both the transverse and longitudinal directions. Their findings indicated that the inter-particle spacing between aggregates in specimens compacted with the vibrating hammer was approximately 8.9 mm [4]. The improved packing density resulting from the vibration-assisted compaction contributed significantly to the higher compressive strength observed in the laboratory specimens compared to RCC pavement (RCCP) produced under field conditions [8].

In contrast, specimens compacted using the Proctor hammer exhibited larger inter-particle spacing, as this method relied solely on impact force without the assistance of vibration. Selvam et al. [4] reported that the inter-particle spacing in specimens compacted by the Proctor hammer was approximately 9.5 mm. The larger spacing led to a lower packing density, which in turn reduced the compressive strength of the specimens compared to those compacted with the vibrating hammer. However, as noted by Selvam et al. [8], the compressive strength of the Proctor hammer-compacted specimens more closely matched the strength of RCCP produced in field conditions.

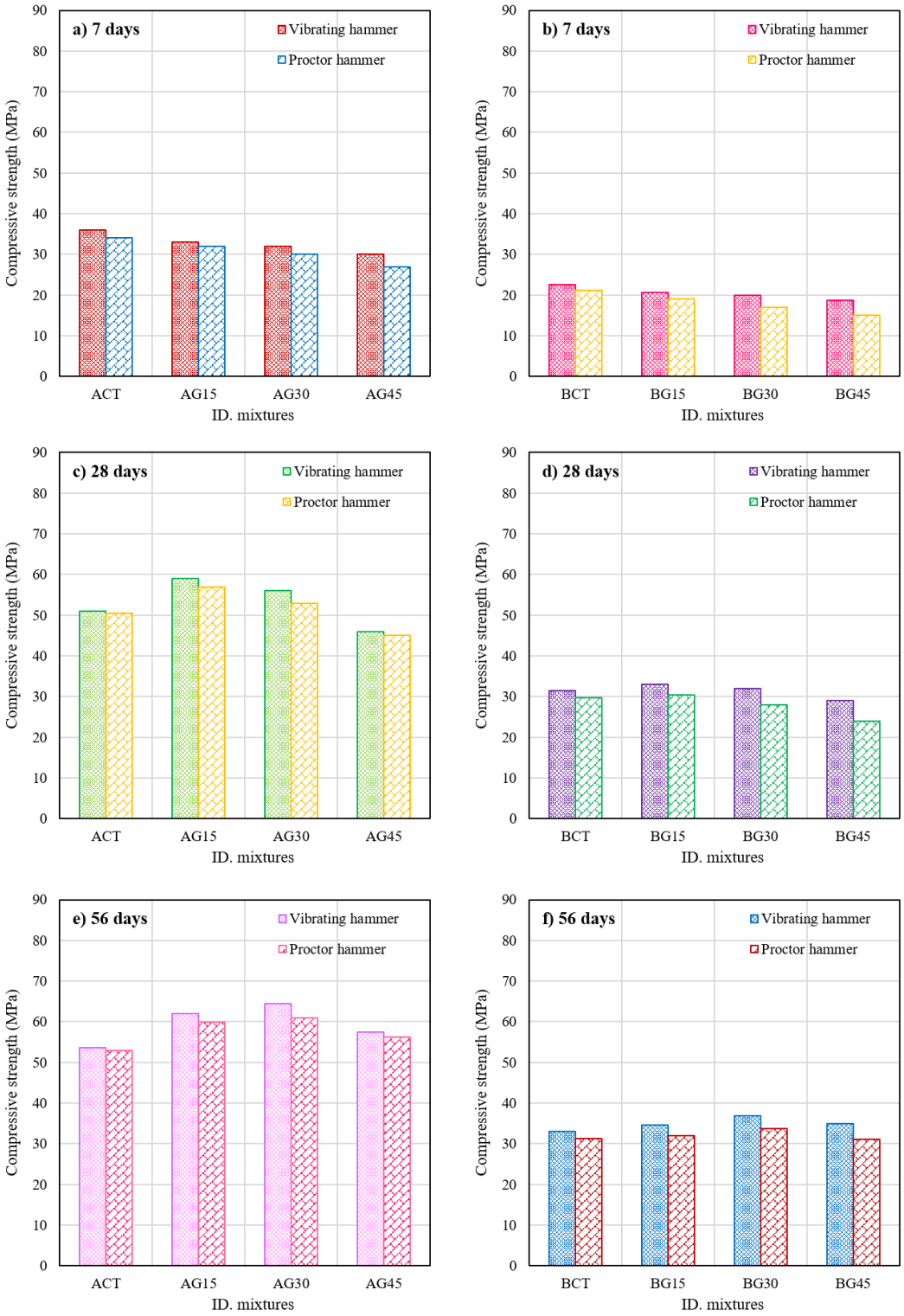

Figure 11. Compressive strength of RCC prepared by Vibrating and Proctor hammer method.

3.4. Effects of the compaction energy on the compressive strength of RCC

As shown in Fig. 12, an increase in compaction energy led to a slight decrease in the compressive strength of RCC specimens. For example, the 28-day compressive strength of the ACT mixture compacted with 30 blows reached 50 MPa, whereas the strength decreased to 49

MPa when compacted with 60 blows. Similar trends were also observed in the AG15, AG30, and AG45 mixtures. Two factors may account for this behavior. Firstly, Sengun et al. [5] reported that the compressive strength of concrete is minimally affected when the compaction ratio exceeds 96%. Secondly, Selvam et al. [4] observed that excessive impact force during compaction, such as from the Proctor hammer, could cause aggregate breakage. Their study reported a significant increase in the amount of material passing through the 4.75 mm sieve, which was attributed to the breakage of larger aggregates under high compaction energy. The alteration of the aggregate size distribution due to breakage likely disrupted the optimal packing structure, leading to a slight reduction in compressive strength.

In contrast, the BCT mixture exhibited an increase in strength with higher compaction energy. This outcome may be attributed to the compaction energy being sufficient to achieve the required strength. Robalo et al. [26] reported that low-cement concrete demands high compaction energy. They observed a 52% increase in compressive strength for low-cement concrete (250 kg of cement per metric ton) compacted with high energy, compared to the control. However, for the BG15, BG30, and BG45 mixtures, the compressive strength decreased when compacted with 60 blows compared to 30 blows. This reduction may be due to the application of compaction energy beyond the optimal level. Since RCC mixtures incorporating GGBFS exhibit higher workability, they require less compaction energy to achieve maximum strength. This result is similar to the trend observed in Group A.

Conversely, when the number of blows was lower than the standard compaction level, the compressive strength of the RCC mixtures also decreased. Inadequate compaction increased the porosity of the RCC, which in turn reduced its strength.

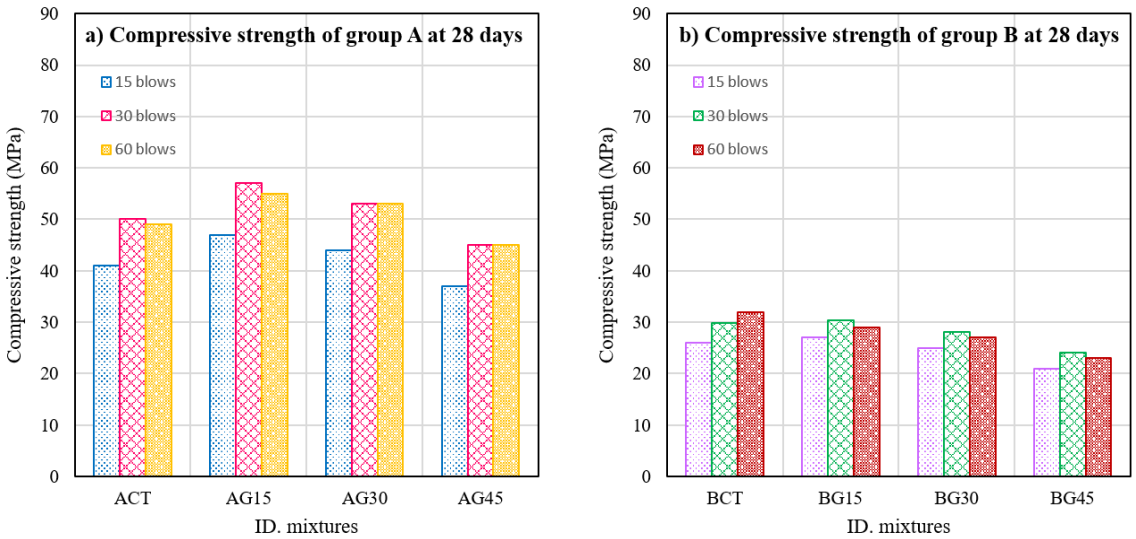

Fig. 12 Compressive strength of RCC compacted by a Proctor hammer with different blows.

4. CONCLUSIONS

Based on the experimental results, the following conclusions can be drawn:

1) The replacement of cement with GGBFS reduced the compressive strength of RCC at 7 days due to the slower reactivity of GGBFS at early ages. However, an improvement in compressive strength was observed at later ages (28 and 56 days). The RCC mixture containing 15% GGBFS achieved the highest compressive strength at 28 days, while the mixture with 30% GGBFS substitution reached the highest strength at 56 days.

2) The RCC specimens compacted using a vibrating hammer exhibited higher compressive strength compared to those compacted with a Proctor hammer. This was attributed to the enhanced aggregate distribution and denser packing achieved through the combined effect of vibration and impact force. In contrast, specimens compacted using the Proctor hammer exhibited larger inter-particle spacing, as this method relied solely on impact force without the assistance of vibration.

3) An increase in compaction energy slightly decreased the compressive strength of RCC in group A. This reduction was likely due to aggregate breakage under excessive compaction, which altered the aggregate size distribution and disrupted the optimal packing structure. In contrast, RCC with a low cement dosage (Group B) requires higher compaction energy, resulting in an increase in compressive strength for BCT specimens compacted with 60 blows. However, the reduction in strength observed in BG15, BG30, and BG45 compacted with 60 blows may be attributed to the application of compaction energy beyond the optimal level.

4) Insufficient compaction energy (15 blows) led to increased porosity, which consequently resulted in a reduction in compressive strength of all mixtures.

ACKNOWLEDGMENT

This research is partly funded by the Vietnam National Foundation for Science and Technology Development (NAFOSTED) under grant number 107.01-2023.06.

REFERENCES

[1]. M. Selvam, K. NSSP, R. Kannan, S. Singh, Assessing the effect of different compaction mechanisms on the internal structure of roller compacted concrete, Constr. Build. Mater, 365 (2022) 130072. https://doi: 10.1016/j.conbuildmat.2022.130072

[2]. E. Sengun, B. Alam, R. Shabani, I. O. Yaman, The effects of compaction methods and mix parameters on the properties of roller compacted concrete mixtures, Constr. Build. Mater, 228 (2019) 116807. https://doi: 10.1016/j.conbuildmat.2019.116807

[3]. S. G. Williams, Comparison of the Superpave Gyratory and Proctor Compaction Methods for the Design of Roller-Compacted Concrete Pavements, Transp. Res. Rec. J. Transp. Res. Board, 1557 (2013) 106–112, https://doi: 10.3141/2342-13

[4]. ASTM C1435/C1435M-08, Standard Practice for Molding Roller-Compacted Concrete in Cylinder Molds Using a Vibrating Hammer, 2008.

[5]. M. Selvam, S. Singh, Comparative investigation of laboratory and field compaction techniques for designing roller compacted concrete pavements (RCCP), Int. J. Pavement Eng., 24 (2023) 2177850. https:// doi: 10.1080/10298436.2023.2177850

[6]. A. Oner, S. Akyuz, An experimental study on optimum usage of GGBS for the compressive strength of concrete, Cem. Concr. Compos., 29 (2007) 505–514. https://doi: 10.1016/j.cemconcomp.2007.01.001

[7]. S. K. Rao, P. Sravana, T. C. Rao, Abrasion resistance and mechanical properties of Roller Compacted Concrete with GGBS, Constr. Build. Mater., 114 (2016) 925–933, https://doi: 10.1016/j.conbuildmat.2016.04.004

[8]. A. Aghaeipour and M. Madhkhan, Effect of ground granulated blast furnace slag (GGBFS) on RCCP durability, Constr. Build. Mater, 141 (2017) 533-541. https://doi: 10.1016/j.conbuildmat.2017.03.019

[9]. ASTM C150-07, Standard Specification for Portland Cement, 2007.

[10]. ASTM C109/C109M-08, Standard Test Method for Compressive Strength of Hydraulic Cement Mortars (Using 2-in or [50-mm]Cube Specimens), 2008.

[11]. ASTM C204-07, Standard Test Methods for Fineness of Hydraulic Cement by Air-Permeability Apparatus, 2007.

[12]. ASTM C191-08, Standard Test Methods for Time of Setting of Hydraulic Cement by Vicat Needle, 2008.

[13]. TCVN 11586-2016, Ground granulated blast-furnace slag for concrete and mortar, 2016.

[14]. American Concrete Pavement Association, Roller-Compacted Concrete Pavements as Exposed Wearing Surface, 2014.

[15]. D. Harrington, F. Abdo, W. Adaska, C. Hazaree, Guide for Roller-Compacted Concrete Pavements," Inst. Transp. Iowa state univerisity, 8 (2010) 104. https://trid.trb.org/view.aspx?id=1082276

[16]. M. Hashemi, P. Shafigh, M. Rehan, B. Karim, C. Duran, The effect of coarse to fine aggregate ratio on the fresh and hardened properties of roller-compacted concrete pavement, Constr. Build. Mater., 169 (2018) 553–566, https://doi: 10.1016/j.conbuildmat.2018.02.216

[17]. ASTM D1557-12, Standard Test Methods for Laboratory Compaction Characteristics of Soil Using Modified Effort (56,000 ft-lbf/ft^3 (2,700 kN-m/m^3)), 2012.

[18]. TCVN 3118-2022, Hardened concrete – Test method for compressive strength, (2022).

[19]. H. Wan, Z. Shui, Z. Lin, Analysis of geometric characteristics of GGBS particles and their influences on cement properties, Cem. Concr. Res., 34 (2004) 133–137. https://doi: 10.1016/S0008-8846(03)00252-7

[20]. S. Tavasoli, M. Nili, B. Serpoosh, Effect of GGBS on the frost resistance of self-consolidating concrete, Constr. Build. Mater., 165 (2018) 717–722. https://doi: 10.1016/j.conbuildmat.2018.01.027

[21]. P. J. Wainwright, N. Rey, The influence of ground granulated blastfurnace slag (GGBS) additions and time delay on the bleeding of concrete, Cem. Concr. Compos., 22 (2000) 253–257. https://doi.org/10.1016/S0958-9465(00)00024-X

[22]. B. Kolani, L. Buffo-lacarrière, A. Sellier, G. Escadeillas, L. Boutillon, L. Linger, Hydration of slag-blended cements, Cem. Concr. Compos., 34 (2012) 1009–1018. https://doi: 10.1016/j.cemconcomp.2012.05.007

[23]. C. M. Yun, M. R. Rahman, C. Y. W. Phing, A. W. M. Chie, M. K. Bin Bakri, The curing times effect on the strength of ground granulated blast furnace slag (GGBFS) mortar, Constr. Build. Mater., 260 (2020) 120622. https"// doi: 10.1016/j.conbuildmat.2020.120622

[24]. C. Hwang, Strength development of blended blast - furnace slag - cement mortars, J. Chinese Institue Eng., 9 (1986) 233–239. https://doi: 10.1080/02533839.1986.9676884

25]. E. Guneyisi, M. Gesoglu, A study on durability properties of high-performance concretes incorporating high replacement levels of slag, Mater. Struct., 41 (2008) 479–493. https://doi: 10.1617/s11527-007-9260-y

[26]. K. Robalo, E. Soldado, H. Costa, H. Alves, E. Júlio, Efficiency of cement content and of compactness on mechanical performance of low cement concrete designed with packing optimization, Constr. Build. Mater., 266 (2021) 121077. https://doi: 10.1016/j.conbuildmat.2020.121077